Large and Stable Refractive Index Change in Photochromic Hybrid Materials

John Biteau, Frédéric Chaput, Khalid Lahlil, and Jean-Pierre Boilot*

Groupe de Chimie du Solide, Laboratoire de Physique de la Matière Condensée, UMR CNRS 7643, Ecole Polytechnique, 91128 Palaiseau, France

Gerasimos M. Tsivgoulis and Jean-Marie Lehn

Collège de France, Chimie des Interactions Moléculaires, UPR CNRS 285, 11 place Marcelin Berthelot, 75231 Paris Cedex 05, France

Bruno Darracq, Chantal Marois, and Yves Lévy

Groupe d'Optique Non Linéaire, Institut d'Optique Théorique et Appliquée, URA CNRS 14, Bâtiment 503, B.P. 147, 91403 Orsay Cedex, France

Received February 25, 1998. Revised Manuscript Received May 8, 1998

We have developed new transparent photochromic hybrid organic−inorganic materials in which the photochromic group belongs to the polymer network. These materials involving chemically bonded dithienylethene derivatives were prepared by the sol−gel process in the form of thin films a few microns thick. The thickness and refractive index of the sol−gel films either at 633 or 785 nm were determined both in the colored and discolored state by using the attenuated total reflection (ATR) method. Functionalized sol−gel films showed a large refractive index change in a nonabsorbing spectral region: $\Delta n \approx 4 \times 10^{-2}$ at 785 nm. This important variation due to the high photochrome content allowed us to design optical components used in the field of wave guiding.

Introduction

The sol−gel technique provides an attractive, low-temperature approach to the preparation of hybrid organic−inorganic matrixes.[1] The chemistry involved in the sol−gel technique is based on the sequential hydrolysis and condensation of alkoxides (usually silicon alkoxides) initiated by an acidic or a basic aqueous solution in the presence of a cosolvent. Depending on the nature of the precursor, inorganic or hybrid organic−inorganic gels are formed, which can be dried to produce xerogels. The mild synthesis conditions offered by the sol−gel route allow for the incorporation of optically active organic molecules (laser dye, second-order nonlinear chromophore, reverse saturable absorber, photochromic molecule, etc.) into the glassy matrix to form doped xerogels with specific optical properties.[2] A variety of shapes, including thin films and monoliths can be prepared. They exhibit good optical qualities (high transmission in visible range) and mechanical strength (easy processing) required for optical applications.

Dithienylethenes are photochromic molecules (Scheme 1) characterized by a large change in their UV−visible absorption spectrum, a thermal irreversibility for most of them, and a high durability for recycle use.[3] They are good candidates for the elaboration of devices exhibiting photoswitched properties such as light absorption,[4] fluorescence,[5] saccharide tweezing,[6] electronic conduction,[7] and light refraction[8] The photoinduced electrocyclization [from the **1-o** (open) form to the **1-c** (closed) one], responsible for the increase in the electronic delocalization of the molecule, also generates an increase of the polarizability of the electronic cloud of the photochromes. They are then able to change the refractive index of the medium in which they are incorporated[9]

(1) Brinker, C. J.; Scherer, G. *Sol−gel science, the physics and chemistry of sol−gel processing*; Academic Press: London, 1990. Special Issue: Sol−Gel Derived Materials. *Chem. Mater.* **1997**, *9* (11).

(2) Boilot, J.-P.; Chaput, F.; Gacoin, T.; Malier, L.; Canva, M.; Brun, A.; Levy, Y.; Galaup, J.-P. *C. R. Acad. Sci. Paris* **1996**, *322*, Série IIb, 27. Avnir, D.; Levy, D.; Reisfeld, R. *J. Phys. Chem.* **1984**, *88*, 5956. Levy, D.; Avnir, D. *J. Phys. Chem*., **1988**, *92*, 4734. Biteau, J.; Chaput, F.; Boilot, J.-P. *J. Phys. Chem.* **1996**, *100*, 9024. Schaudel, B.; Germeur, C.; Sanchez, C.; Nakatami, K.; Delaire, J. A., *J. Mater. Chem.* **1997**, *7 (1)*, 61. Levy, D. *Chem Mater.* **1997**, *9*, 2666.

(3) Irie, M.; Mohri, M. *J. Org. Chem.* **1988**, *53*, 803. Nakamura, S.; Irie, M. *J. Org. Chem.* **1988**, *53*, 6136.

(4) a) Irie, M.; Miyatake, O.; Uchida, K.; Eriguchi, T. *J. Am. Chem. Soc.* **1994**, *116*, 9894. b) Kawai, S. H.; Gilat, S. L.; Ponsinet, R.; Lehn, J.-M. *Chem. Eur. J.* **1995**, *1*, 285.

(5) Tsivgoulis, G. M.; Lehn, J.-M. *Angew. Chem., Int. Ed. Engl.* **1995**, *34*, 1119.

(6) Takeshita, M.; Uchida, K.; Irie, M. *Chem. Commun.* **1996**, 1807. Takeshita, M.; Irie, M. *Tetrahedron Lett.* **1998**, *39* (7), 613.

(7) Tsivgoulis, G. M.; Lehn, J.-M. *Adv. Mater.* **1997**, *9*, 39. Gilat, S. L.; Kawai, S. H.; Lehn, J.-M. *Chem. Eur. J.* **1995**, *1*, 275.

(8) Tanio, N.; Irie, M. *Jpn. J. Appl. Phys.* **1994**, *33*, 1550. Yoshida, T.; Arishima, K.; Ebisawa, F.; Hoshino, M.; Sukegawa, K.; Ishikawa, A.; Kobayashi, T.; Hanazawa, M.; Horikawa, Y. *J. Photochem. Photobiol. A: Chem.***1996**, *95*, 265.

(9) Tanio, N.; Irie, M. *Jpn. J. Appl. Phys.* **1994**, *33* , 3942. Hoshino, M.; Ebisawa, F.; Yoshida, T.; Sukegawa, K. *J. Photochem. Photobiol. A: Chem.* **1997**, *105*, 75.

S0897-4756(98)00106-9 CCC: $15.00
Published on Web 06/19/1998

Scheme 1

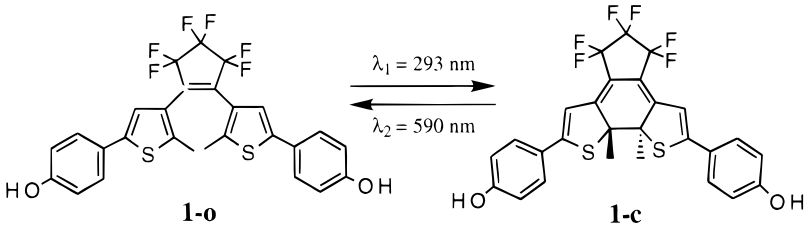

Scheme 2

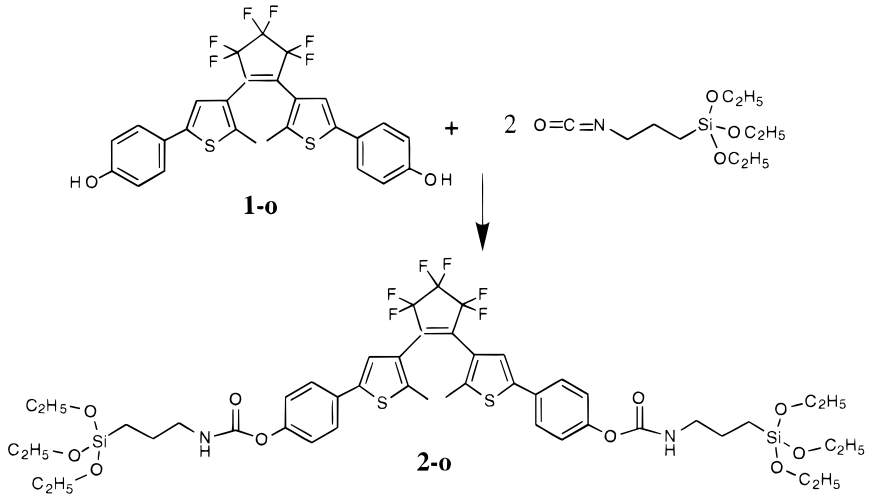

We have already reported the preparation and the study of hybrid organic−inorganic xerogels doped with dithienylethene derivatives.[10] We showed that the sol−gel films exhibited a large refractive index change ($\Delta n = 3 \times 10^{-3}$ at 785 nm) considering the low doping level (0.7 wt %). But the low solubility of the dithienylethenes in the sol−gel medium prevents the refractive index change from being increased. To overcome this limit, the photoactive molecules can be functionalized with trialkoxysilyl groups, allowing the copolymerization with a sol−gel molecular precursor and consequently the grafting of active molecules on the gel network.[11]

In this paper we report the synthesis of a triethoxysilylated dithienylethene derivative and the preparation of sol−gel materials based on the cocondensation between the hydrolyzed species of this functionalized photochrome and of the methyltriethoxysilane ($CH_3Si(OEt)_3$/MTEOS) precursor. The hybrid organic−inorganic thin films exhibit a large refractive index change after UV irradiation. This allows us to inscribe gratings and various patterns by using the photomask technique.

Experimental Section

Synthesis of a Silylated Dithienylethene. 1,2-Bis[5′-(4″-hydroxyphenyl)-2′-methylthien-3′-yl]perfluorocyclopentene (**1**), the formula of which is shown in Scheme 1, was used as a raw material to prepare the photochromic functionalized monomer **2-o**. A detailed procedure of its synthesis has been previously reported in ref 4b. The silylated dithienylethene molecule was prepared in conformity with the published procedure (Scheme 2).[12] The hydroxyl groups of the photochromic dye reacted with the isocyanate group of the silicon precursor. A mixture of 105.3 mg (0.19 mmol) of **1**, 53.7 μL (0.38 mmol) of triethylamine, and 146 μL (0.57 mmol) of 3-isocyanatopropyltriethoxysilane in 3.5 mL of anhydrous tetrahydrofuran was stirred for 7 h under nitrogen atmosphere at 72 °C. After cooling, the solvent and triethylamine were evaporated. The whole amount of **1** reacted and the excess 3-isocyanatopropyltriethoxysilane was eliminated by recrystallization in hexane. A 161.6 mg (0.15 mmol, yield 81%) portion of bluish powder was obtained. ^{1}H NMR spectra were recorded on a Brucker WP200 spectrometer (200 MHz) using $CDCl_3$ as solvent. The NMR resonances of monomer **2** (**2-o** and **2-c** forms) are reported in ref 13. Infrared experiments were monitored in CCl_4, on a Bomem FTIR spectrometer with a DTGS detector. UV−vis spectra were recorded using a Shimadzu UV−vis 160A spectrophotometer. The UV−vis

Table 1. Absorption Spectral Data for Compounds 1 and 2

molecule	λ_{max}/nm ($\epsilon \times 10^{-4}$/mol^{-1} L cm^{-1})
1-o[a]	293 (3.8)
1-c[a]	340 (2.5), 590 (1.8)
2-o[b]	290 (3.5)
2-c[b]	315 (2.6), 381 (1.1), 587 (1.6)

[a] In CD_3CN.[4b] [b] In $CDCl_3$.

(10) Biteau, J.; Tsivgoulis, G. M.; Chaput, F.; Boilot, J.-P.; Gilat, S.; Kawai, S.; Lehn, J.-M.; Darracq, B.; Martin, F.; Lévy, Y. *Mol. Cryst. Liq. Cryst.* **1997**, *297*, 65.

(11) Chaput, F.; Riehl, D.; Boilot, J.-P.; Cargnelli, K.; Canva, M.; Levy, Y.; Brun, A. *Chem. Mater.* **1996**, *8*, 312. Lebeau, B.; Sanchez, C.; Brasselet, S.; Zyss, J.; Froc, G.; Dumont, M. *New J. Chem.* **1996**, *20*, 13. Nakashima, H.; Irie, M. *Macromol. Rapid Commun.***1997**, *18 (8)*, 625.

(12) Chaput, F.; Riehl, D.; Lévy, Y.; Boilot, J.-P. *Chem. Mater.* **1993**, *5*, 589.

(13) Multiplicities are given as s (singlet), d (doublet), t (triplet), q (quartet), and m (multiplet). ^{1}H NMR (200 MHz, $CDCl_3$): **2-o**: δ = 0.69 (m, 4H, C**H$_2$**Si), 1.25 (t, 18H, C**H$_3$**CH$_2$OSi), 1.72 (m, 4H, CH$_2$C**H$_2$**-CH$_2$), 1.94 (s, 6H, 2′-C**H$_3$**), 3.28 (m, 4H, NHC**H$_2$**), 3.84 (q, 12H, CH$_3$C**H$_2$**-OSi), 5.32 (t, 2H, N**H**CH$_2$ *and rotational conformer at 4.88*), 7.14 (d, 4H, H-2″,6″), 7.21 (s, 2H, H-4′), 7.51 (d, 4H, H-3″,5″); **2-c**: δ = 0.69 (m, 4H, C**H$_2$**Si), 1.25 (t, 18H, C**H$_3$**CH$_2$OSi), 1.72 (m, 4H, CH$_2$C**H$_2$**CH$_2$), 2.16 (s, 6H, 2′-C**H$_3$**), 3.28 (m, 4H, NHC**H$_2$**), 3.84 (q, 12H, CH$_3$C**H$_2$**OSi), 5.32 (t, 2H, N**H**CH$_2$ *and rotational conformer at 4.88*), 7.19 (d, 4H, H-2″,6″), 6.62 (s, 2H, H-4′), 7.56 (d, 4H, H-3″,5″).

Scheme 3

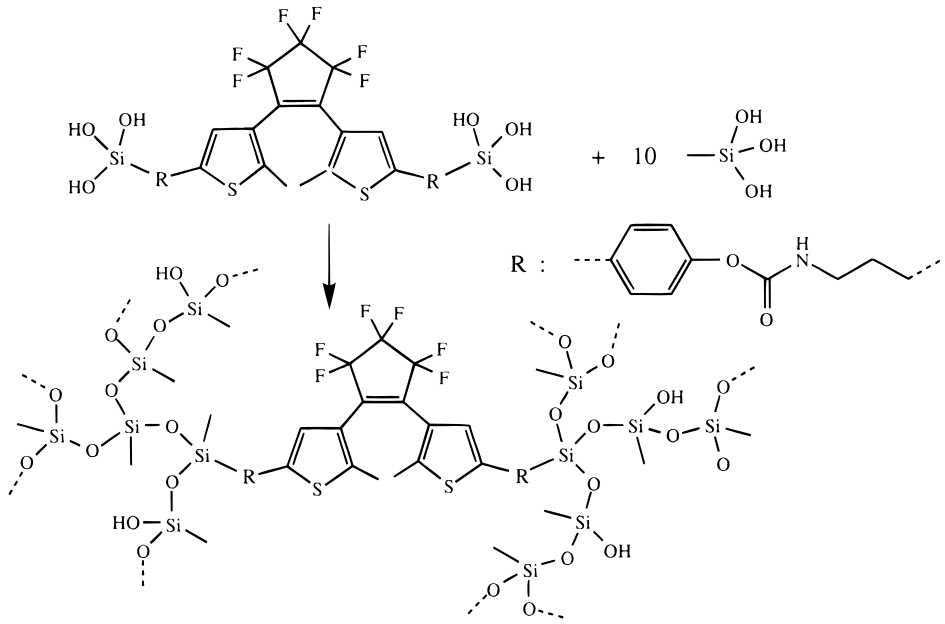

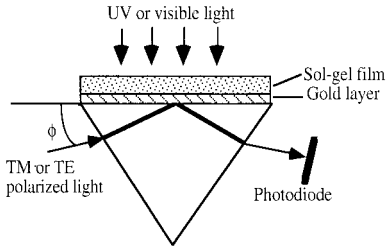

Figure 1. Kretschmann's configuration of ATR experiment

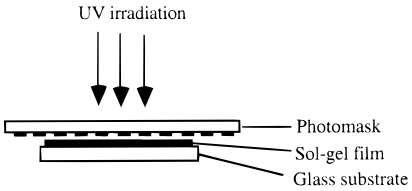

Figure 2. Experimental setup used to inscribe high-refractive-index waveguide patterns.

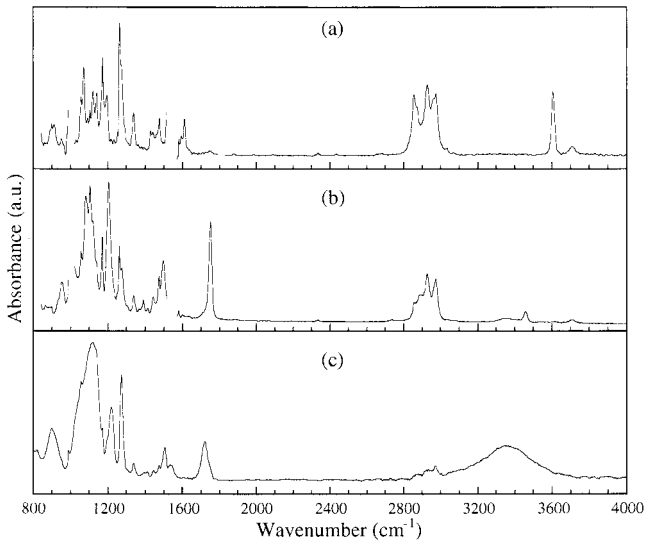

Figure 3. Infrared spectra of (a) **1-o** in a CCl_4 solution, (b) **2-o** in a CCl_4 solution (blank spaces correspond to the peaks of the solvent), and (c) a thin film of **2-o**/MTEOS freshly deposited on a crystalline silicon (c-Si) wafer.

spectroscopy data of **1** and **2** are listed in Table 1. The molar extinction coefficient for the **2-o** form was directly deduced from the absorbance of a 3.9×10^{-5} M solution in $CDCl_3$. Concerning the **2-c** form, the molar extinction coefficients were calculated from the absorbance of the previous solution after partial coloration by UV irradiation. The percentage of the **2-c** form (46%) in this solution was then deduced from the ^1H NMR spectrum.

Sol−gel Preparation of the Hybrid Films. To obtain solid-state photochromic materials, the functionalized dithienylethene was copolymerized with methyltriethoxysilane (Scheme 3).[11] In a typical sol preparation, 81.8 mg (0.078 mmol) of **2-o** was dissolved in 1 mL of tetrahydrofuran. A 0.156 mL (0.78 mmol) portion of methyltriethoxysilane was added before introduction of 59 μL of acidic water (pH 1). After 1 h of magnetic stirring, pyridine (59 μL) was added to neutralize the acidity of the medium and therefore to increase the condensation reaction rate. Afterward, the so-prepared hybrid sol was passed through a 0.45 μm filter before deposition. The viscous sol was poured onto the substrates for spin coating. The angular velocity range of the spinner was 1000−4000 rpm. Thin films (0.45 and 0.64 μm of thickness) were spin-coated on various substrates. Plain glass substrates were used for UV−visible absorption experiments, some of them were previously gold coated by thermal evaporation for thickness and refractive index measurements. These sample plates were finally heated at 70 °C for 15 h. For FTIR measurements the films were deposited on single crystalline silicon substrates (c-Si) and underwent variable thermal treatments. To avoid interference fringes on the transmission spectra of the films due to multiple reflections in the hybrid film, we used p-polarized infrared light at oblique incidence (Brewster's angle = 60°).[14]

Determination of the Thickness and the Refractive Index of the Sol−Gel Films. The ATR experiment is a well-known method for measuring indices and the thickness of transparent thin films.[15] This technique is a generalization of the Kretschmann method using surface plasma wave propagation on a metallic surface.[16] It allows the excitation of the guided modes supported by the thin film by a resonant coupling with a free wave, through a metallic layer. Resonance

(14) Harrick, N. J. *Appl. Spectrosc.* **1997**, *31* (6), 548.
(15) Dumont, M.; Lévy, Y.; Morichère, D. In *Organic Molecules for NonLinear Optics and Photonics;* Messier, J., Ed.; Kluwer Academic Publishers: Boston, 1991; p 461.

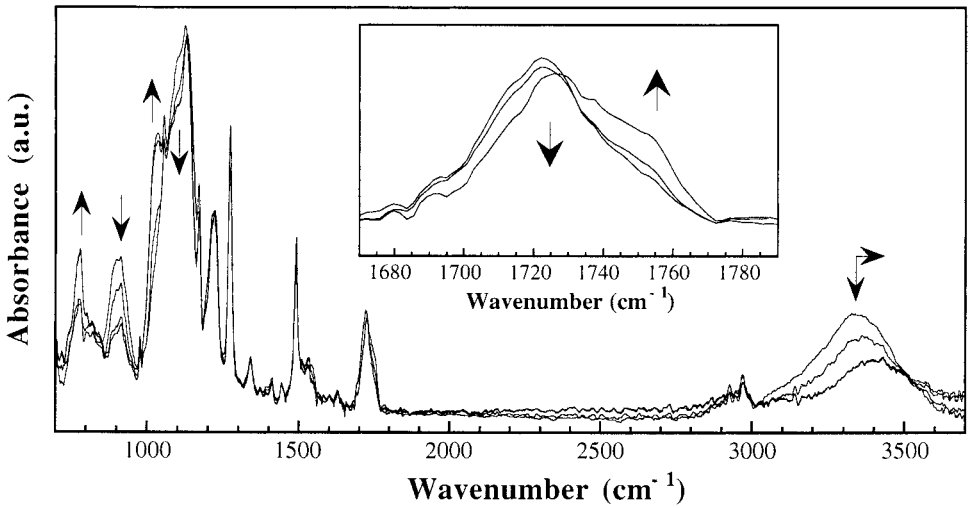

Figure 4. Infrared spectra of a **2-c**/MTEOS colored thin film deposited on a c-Si wafer illustrating the condensation of silanols into siloxanes during the drying process (a similar evolution is observed for **2-o**/MTEOS thin films). The spectra are those of a film dried at room temperature, 15 h at 70 °C, 1 h at 130 °C, and 2 h at 130 °C. The inset shows the influence of silanol hydrogen bonds on the carbamate vibration mode: The contribution of hydrogen-bonded carbamates at 1725 cm^{-1} decreases while the contribution of non-hydrogen-bonded carbamates at 1752 cm^{-1} increases.

conditions allow accurate determination of the refractive index (accuracy < 10^{-3}) and the thickness and are very sensitive to any changes occurring inside or at the surface of the film. Figure 1 shows the experimental setup. A thin metallic gold layer (≈42 nm) is deposited on the base of a glass prism (n = 1.5095 at 785 nm) and overlayered with the xerogel film to be studied. A collimated monochromatic light beam emitted from a He−Ne laser (wavelength 633 nm) or a laser diode (785 nm) is reflected on the multilayered structure (through the prism) and the reflectivity R is measured versus incidence angle (external angle Φ). As the waveguide resonance relation is fulfilled, the incident wave is coupled with one of the guided modes in the dielectric film. The reflectivity curve exhibits a set of dips related to the transverse resonance condition: $2k_{mz}h + \psi_1 + \psi_2 = 2m\pi$, where k_{mz} is the normal component of the wave vector, h is the film thickness, m is the order of the guided mode (an integer), and ψ_1 and ψ_2 are the phase shifts at reflection on the inner faces of the waveguide. They are calculated from the Fresnel coefficients and thus depend on the light polarization. Therefore, there are two sets of polarized modes: TM (transverse magnetic) and TE (transverse electric). From the precise angular position measurements Φ_m of the reflectivity minima, the refractive index and the thickness of the xerogel film are determined by using the resonance condition.

Pattern Inscription and Illumination Conditions. The percentages of conversion from **2-o** to **2-c** at the photostationary state both in $CDCl_3$ and in the gel matrix were estimated from the maximum of coloration obtained by pure UV irradiation and using the molar extinction coefficients calculated for the pure **2-c** form in $CDCl_3$ solution.

In addition, the photochromic properties of the dithienylethene sol−gel films were used for writing channel waveguides, gratings, and others patterns used in integrated optics. As shown in Figure 2, the photochrome-containing xerogel films previously discolored by an expanded argon laser beam at 514 nm were colored through a mask by UV irradiation. In this case, for practical accommodations, the UV lamp (312 nm) used for the film irradiation also emitted visible light. Then for all these experiments the coloration rate of the films was only about 80%.

Results

The silylation previously described has been followed by infrared spectroscopy and could be mainly characterized[17] by comparing the spectra a and b in Figure 3, by the disappearance of the O−H stretching vibration at 3605 cm^{-1} and also by the appearance of the asymmetric stretching modes of Si−O−C at 1082 and 1103 cm^{-1}, the amide IV band (combination of C−N and C−O stretching) at 1203 cm^{-1}, and the stretching vibration of the C═O at 1752 cm^{-1}. The silylated photochrome **2** was then used to prepare a sol with MTEOS (noted **2-o**/MTEOS). The state of condensation of this sol can be qualitatively seen from the IR spectrum recorded on a freshly deposited thin film (Figure 3c), which shows the hydrolysis of ethoxysilanes with the Si−O(H) stretching mode at 900 cm^{-1} and the (Si)O−H stretching mode around 3340 cm^{-1}. The partial condensation also appears with the Si−O−Si asymmetric stretching modes between 1030 and 1150 cm^{-1}.

The condensation of the **2**/MTEOS thin film (**2-o** and **2-c** forms) during the heating process was then followed by infrared spectroscopy (Figure 4). Two of the direct spectral consequences of the condensation into siloxanes Si−O−Si are the decrease of the Si−O(H) stretching mode at 900 cm^{-1} and of the (Si)O−H stretching mode at 3340 cm^{-1}. Hydrogen bonding on silanols lowers the (Si)O−H stretching energy. The shift of the band maximum from 3340 to 3400 cm^{-1} is explained by the decrease of the concentration of hydrogen-bonded silanols which first condensate into siloxanes. Another direct consequence of the condensation is the increase of the asymmetric Si−O−Si stretching vibration contribution at 1025 cm^{-1}. It is accompanied by a decrease of a contribution around 1105 cm^{-1}, which could be attributed to species containing both siloxanes and silanols.[18] The symmetric Si−O−Si stretching mode was also followed at 780 cm^{-1}. Besides, the inset in Figure 4 shows the shift of the C═O stretching carbamate band, along with the condensation, from 1725 to

(16) Kretschmann, E.; Raether, H. *Z. Naturf.* **1968**, *23a*, 2135.

(17) Socrates, G. *Infrared Characteristic Group Frequencies*; J. Wiley & Sons: New York, 1980. Lin-Vien, D.; Colthup, N. B.; Fateley, W. G.; Grasselli, J. G. *The Handbook of Infrared and Raman Characteristic Frequencies of Organic Molecules*; Academic Press: San Diego, 1991. Ou, D. L.; Seddon, A. B. *J. Non-Cryst. Solids* **1997**, *210*, 187.

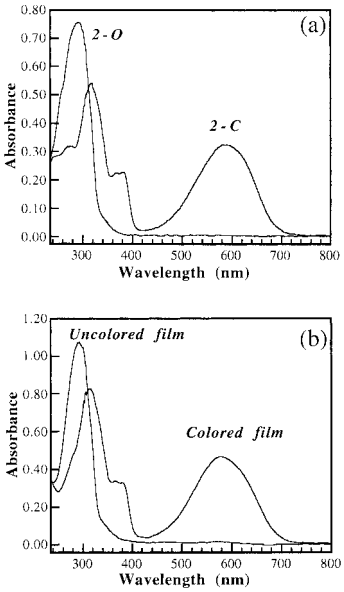

Figure 5. (a) UV−vis electronic absorption spectra of the open and closed forms of **2** in $CDCl_3$ solution (1.1×10^{-4} mol/l) for a path length of 0.2 cm. The spectrum of **2-c** corresponds to a solution with a conversion rate ≥ 93%. (b) UV−vis electronic absorption spectra of uncolored and colored **2**/MTEOS hybrid films. The colored photostationnary state corresponds to a conversion rate of 95%, considering that ϵ is unchanged by the environment (from $CDCl_3$ to hybrid film).

1752 cm^{-1}, corresponding to hydrogen-bonded carbamates and non-hydrogen-bonded carbamates, respectively. The films for optical measurements were dried for 15 h at 70 °C. Such films contained a significant amount of residual silanols.

The UV−vis absorption spectra of the photochrome appeared as modified by the silylation of **1** to form **2**, as shown in Table 1 and Figure 5a. For the **2-c** colored form, the introduction of the carbamate function affected the UV part of the spectrum which presents an intense band at 315 nm. However, when comparing the absorption band maximum at 587 nm for **2-c** in $CDCl_3$ and at 590 nm for **1-c** in CD_3CN,[4b] it was observed that the visible band was unchanged. A clear isosbestic point was noted at 311 nm. From the solution of **2** in $CDCl_3$ to the grafted photochrome **2** in the sol−gel matrix, the absorption spectra did not change markedly (Figure 5b). The blue shift of the visible absorption band from 587 nm (**2-c** in $CDCl_3$) to 577 nm (**2-c** grafted to the sol−gel matrix) was assigned to a variation of the polarity of the environment. The enlargement of this band (increasing of 5% of the half-height width) can be explained by the local inhomogeneity of the surrounding medium induced by the nature of the matrix.

A similar value (about 95%) was found in solution and in the gel matrix for the percentage of conversion from **2-o** to **2-c** at the photostationary state (Figure 5). This shows that both the functionalization of the dithienylethene (**1** → **2**) and the incorporation to the hybrid matrix do not significantly modify the conversion rate (98% for **1** molecules[4b]). Weak matrix effects are consistent with the low volume change accompanying the **o** → **c** conversion. In addition, concerning the stability of the **2-c** form, only 6% of thermal discoloration (**2-c** → **2-o**) was observed after heating the colored gel at 100 °C during 24 h.

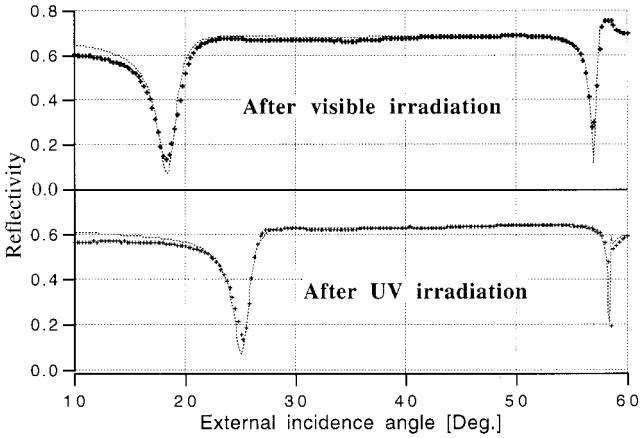

Figure 6. Reflectivity recorded as a function of the external incidence angle for TM polarized light at 785 nm wavelength, after visible and UV irradiation. The crosses represent experimental data and the dotted lines are the theoretical curves obtained from the fitting procedure.

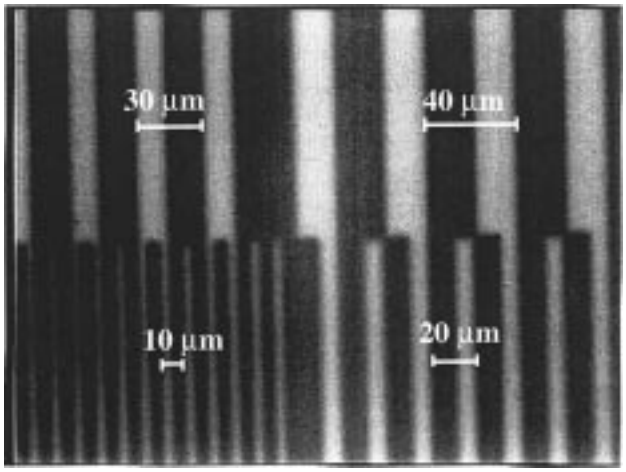

Figure 7. Photomicrograph of gratings revealed on diethienylethene containing **2**/MTEOS sol−gel film after UV irradiation.

Figure 6 shows the experimental reflectivity curve (only for the TM mode) for a **2-o**/MTEOS sol−gel thin film. Measurements were performed at 785 nm, i.e., outside the strong absorption band located around 587 nm. The reflectivity was recorded first when the photostationary state was reached under UV irradiation and second after a strong illumination at 633 nm. As shown in Figure 6, a large angular shift of the reflectivity dips was observed on the reflectivity curves. This shift is mainly due to the change of the real part of the refractive index. The change of the refractive index $\Delta n = 4 \times 10^{-2}$, due to photoconversion from the colorless state ($n = 1.533$) to the colored state ($n = 1.573$), is 1 order higher than previous results obtained with samples having a lower doping level.[10] This large value of the photoinduced Δn is promising for photooptical applications.[8] The film thickness deduced from these experiments was close to 0.65 μm.

Figure 7 shows an optical photomicrograph of gratings revealed on a photochromic sol−gel film after UV irradiation through a photomask supporting four gratings of different periods (10, 20, 30, and 40 μm). The

(18) Brown, J. F. *J. Am. Chem. Soc.* **1965**, *87*, 4317.

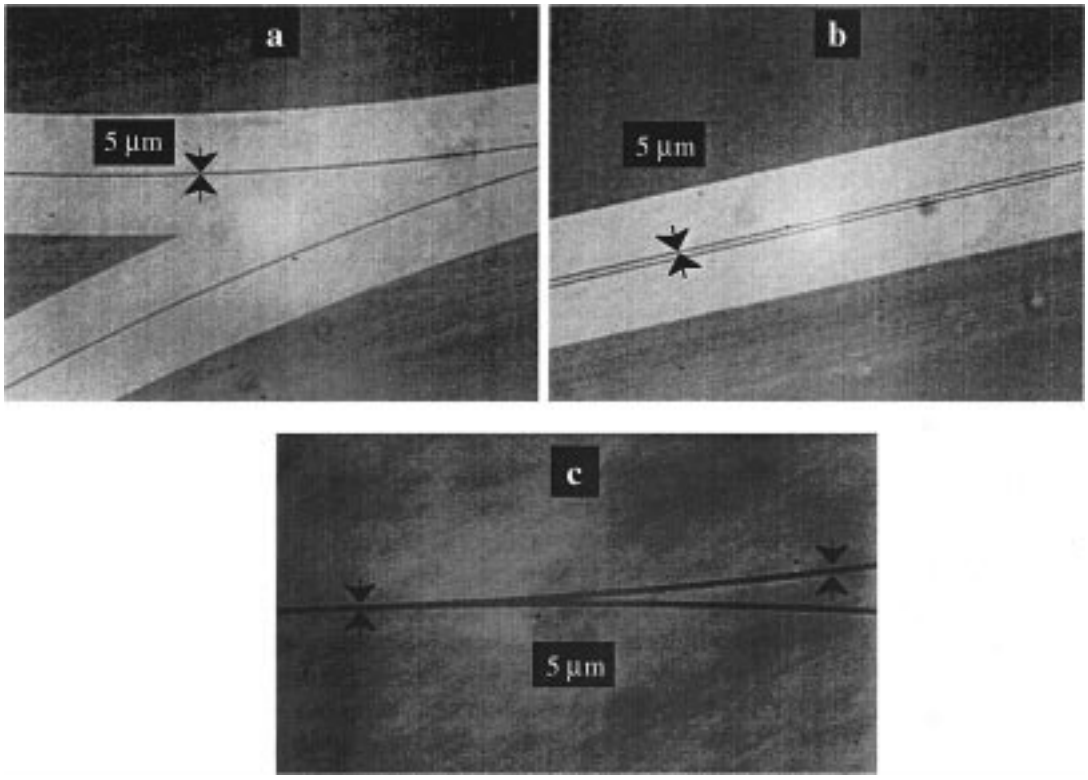

Figure 8. Different configurations for waveguides: (a and b) details of a directional coupler and (c) Y branch of a Mach−Zender interferometer.

photograph was taken 1 day later. The gratings were characterized by measuring the diffraction efficiency of the different patterns at 785 nm. The experimentally measured diffraction efficiency was 10^{-3}, leading to a Δn between colored and discolored states of 3.9×10^{-2}. This value was calculated from the following theoretical formula leading to the diffraction efficiency for a step index grating:

$$\eta = \frac{1}{\left(1 + \frac{\lambda}{\Delta n h}\right)^2}$$

where h is the thickness of the film and λ the wavelength of the probe beam. This value of the photoinduced Δn confirms previously presented ATR results.

Thermally stable photochromic dithienylethene based sol−gel systems have also been used to generate complex high-refractive-index waveguide patterns after UV irradiation of the thin films through the appropriate photomask. The waveguides may be fabricated in different configurations, as illustrated in Figure 8. Figure 8a,b shows details of a directional coupler. A Y branch of a Mach−Zender interferometer is represented in Figure 8c.

Conclusion

In summary, a disubstituted dithienylethene derivative with triethoxysilyl groups was synthesized. We have demonstrated that the use of such a functionalized silicon alkoxide allows the preparation of thin films in which photochromic molecules are covalently attached to the gel network. These materials showed interesting photochromic properties, such as high photochromic reaction efficiency, thermal stability, and strong absorption in the colored state. The thickness and optical index of the photochromic films can be easily deduced from ATR experiments. These hybrid sol−gel systems display a large thermally stable photoinduced refractive index change at 785 nm, 4×10^{-2}, which is at least 1 order of magnitude higher than the values previously observed for other solids containing diarylethene units.[8−10] This allows us to write efficient channel waveguides and gratings. In addition, such a thermally irreversible photochromic material is a potential candidate for application in optically rewritable information storage media.[19]

CM980106H

(19) Biteau, J.; Peretti, J.; Chaput, F.; Safarov, V.; Boilot, J.-P.; Lehn, J.-M., unpublished results.